ECCOMAS

Proceedia

URBAN SETTLEMENTS MONITORING USING EGMS DATA THROUGH ADAFINDER TOOL

Annalisa Mele[1], Michele Crosetto[2], Andrea Miano[1] and Andrea Prota[1]

[1] Department of Structures for Engineering and Architecture, University of Naples "Federico II"
Via Claudio 21, 80125 Naples, Italy
{annalisa.mele, andrea.miano, aprota}@unina.it

[2] Centre Tecnològic de Telecomunicacions de Catalunya (CTTC/CERCA), Geomatics Research Unit
Avinguda Carl Friedrich Gauss, 7, 08860 Castelldefels, Barcelona, Spain
mcrosetto@cttc.cat

Abstract

The Structural Health Monitoring of urban settlements can be pursued today exploiting satellite remote sensing Advanced Differential Synthetic Aperture Radar interferometry (A-DInSAR) techniques. At the European scale, the new European Ground Motion Service (EGMS) gives the deformative information obtained by the processing of the enormous archives of Sentinel-1 Synthetic Aperture Radar (SAR) images in the period 2015-2020. In this work, a new procedure for valuable use of EGMS-derived data aimed at the monitoring of the deformations of urban areas is presented. The procedure includes the exploitation of a tool, called ADAfinder, which is able to extract active deformation areas (ADA) from datasets of measuring points, which means, it creates maps of areas affected by deformations above an estimated threshold. The aim of the procedure is the identification of buildings included in ADA, representing the buildings that require special attention, in terms of on-site monitoring or inspections. An application is presented, regarding a portion of the Zona Franca industrial area, in the city of Barcelona (Spain).

Keywords: Structural Health Monitoring, European Ground Motion Service, A-DInSAR, ADAfinder, deformation maps.

1   INTRODUCTION

The Structural Health Monitoring (SHM) of existing structures at territorial scale is not easy to carry out adopting traditional techniques. In alternative, innovative techniques based on the processing of satellite-derived images are spreading nowadays, with much lower costs [1]. In particular, SHM of urban settlements can be pursued by exploiting satellite remote sensing Advanced Differential Synthetic Aperture Radar interferometry (A-DInSAR) techniques [2]. As proved by recent research [3]-[9], the latter are very valuable for observing ground deformations of large areas and monitoring phenomena of various natures, e.g., subsidence, slow-moving landslides, and settlements induced by excavations or mining activities. However, it is worth noting that satellite radar-based techniques can also be adopted for monitoring single structures when satellite-derived images have an appropriate resolution [10]-[17]. Potential and limitations for structural assessment and monitoring using satellite RADAR interferometry are described in Talledo et al. 2022 [18].

In the last decades, many European Nations have enabled satellite-RADAR-based services for the monitoring of their territories, e.g., Italy [19]-[21], Norway [22], and Germany [23]. In 2017, a turning point has been the approval of the European Ground Motion Service (EGMS) [24] by the Copernicus Land Monitoring Service. The new EGMS gives deformative information obtained by the processing of the enormous archives of Synthetic Aperture Radar (SAR) images acquired by the Sentinel-1 constellation in the period 2015-2020, at the continental scale. The novelty of EGMS is that deformation data are free and open [25].

It is worth noting that the number of data to consider for SHM of a certain area is very huge. Then, it is very important to study new methodologies to best leverage them (e.g., [8],[26]-[29]). In this work, a procedure for a valuable use of EGMS-derived data (or other satellite data) aimed at the monitoring of the deformations of urban areas is presented. The procedure includes the exploitation of a tool, called "ADAfinder", developed by the Research Unit of Geomatics of the Centre Tecnològic de Telecomunicacions de Catalunya (CTTC). It is able to extract active deformation areas (ADA) from datasets of satellite-derived measuring points, which means, it creates maps where the areas affected by deformations above an estimated threshold are identified. The tool is described in Barra et al. [30] and Navarro et al. [31], while an experimental application is reported in Tomás et al. [32]. The procedure proposed in this work has been described in deep in Mele et al. [33]. It aims to the identification of existing buildings included in the detected ADA. The latter represent the buildings requiring attention and priority in terms of inspections and/or on-site monitoring.

The novelty of the work is related, on one side, to the use of the new EGMS data. On the other side, the data are managed and elaborated through a very promising tool, aimed to minimize the number of information to be stored in relation to the number of information entering the system. In addition, the application included in this work represents one of the first applications of the ADAfinder tool in urban areas.

The structure of the paper is the following. Section 2 contains information about the materials and methods, that are, the EGMS data and the ADAfinder tool descriptions. The proposed methodology is illustrated in Section 3. Section 4 presents an application on a case study area in the city of Barcelona (Spain). A discussion on the potential and the limitations of the proposed methodology are discussed in Section 4. Finally, Section 5 is devoted to the conclusions of the work.

2   MATERIALS AND METHODS

In this Section, the main aspects related to the EMGS data and the ADAfinder tool are described.

The satellite data used in the present work have been downloaded by the EGMS. At the moment, EGMS includes data processed using full resolution A-DInSAR [2], obtained from archive images in the period 2015-2020. The images are acquired by Sentinel-1A and 1B satellites, both in ascending (ASC) and descending (DES) orbits. More details about all the features of the EGMS can be found in the White Paper [34].

EGMS includes three levels of products, based on the direction of the considered deformation and the spatial reference. In particular, in this work, the "calibrated" products will be exploited, which are the geocoded measuring points with their deformation history in terms of components of the deformation velocity along the line of sight (LoS, in ASC and DES orbits). These data are integrated with Global Navigation Satellite Systems (GNSS) information, so they are not referred to a local reference point.

ADAfinder is one of the four tools developed by the Research Unit of Geomatics of the Centre Tecnològic de Telecomunicacions de Catalunya (CTTC), called ADAtools [30], [31]. It lets the minimization of the measuring points to be stored based on their deformation velocity value. Thanks to ADAfinder tool it is possible to create maps of ADA extracted from datasets of measuring points referred to an area of interest. The ADA are identified based on some parameters to set, among which the most important one is the threshold value for the mean deformation velocity (V_m) of the area, which is a function of the standard deviation of the velocities of all the measuring points of the area [30]. The measuring points that are not included in an ADA are considered to be "stable" if the velocity value associated with them is lower than the threshold, or "isolated" if there are no other PSs within a defined distance. ADAfinder tool gives two outputs, that are, the polygons representing the ADA, and the PSs included in them.

3   PROPOSED METHODOLOGY

The methodology proposed in this work has been deeply described in Mele et al. [33]. The methodology aims to identify constructions affected by severe deformation velocity, where the severity is established based on the deformation velocity of the whole area under monitoring. The workflow of the methodology is reported in Figure 1.

First of all, preliminary operations are carried out in a GIS software (green box in Figure 1), to filter the data and focus on the constructions included in the ADA. A shapefile containing the polygons of the constructions shapes is required. To exclude the shapes that erroneously could not represent constructions, polygons with small areas (in this case, lower than 30 m^2) are excluded. A buffer of the polygons is performed to consider possible inaccuracies. After these preparation steps, the two datasets of measuring points referred to ASC and DES orbits are imported, and a selection of the measuring points intersecting the previous polygons is done. From this step, all the following steps included in the black contour in Figure 1 must be carried out both for the ASC and the DES datasets, separately. The buildings without measuring points are identified. Then, the ADAfinder tool is performed (yellow box in Figure 1). The stability threshold on the deformation velocity, the ADA radius (in meters), and the minimum number of measuring points to include in an ADA (minimum 3 in the current version) are set. The stability threshold is set at 2σ or 1σ if V_m is lower than σ or greater than σ, respectively. At this step, the ADAfinder tool gives two results (orange box in Figure 1), which are a map of the ADA (a polygonal shapefile), and a map of the measuring points included in every ADA (a point shapefile). The final part of the procedure (blue box in Figure 1) consists of the elaboration of the ADAfinder results. The ADA are overlapped with the polygons of the constructions' shapes. The buildings not contained within an ADA or a portion of an ADA are removed, while the buildings (or portions of them) included in an ADA are classified as "unstable". The measuring points on the unstable buildings are divided into

ASC and DES, as it was originally. Then, for each building covered by an adequate number of measuring points, the average of the V_m of its measuring points is computed, so to have only two values of V_m, one ASC ($V_{m,ASC}$) and one DES ($V_{m,DES}$). The buildings without at least one ADA from both the orbits are excluded, because both are required to estimate the Vertical and East-West (E-W) mean deformation velocity components. Finally, for each building, the Vertical and E-W mean deformation velocity components are estimated according to Talledo et al. [18]. The steps contained in the dotted red contour in Figure 1 are performed separately for each building included in an ADA. Thanks to the Vertical and E-W mean deformation velocity components it is possible to identify constructions affected by significant settlements, that need a more accurate level of SHM with respect to the stable ones.
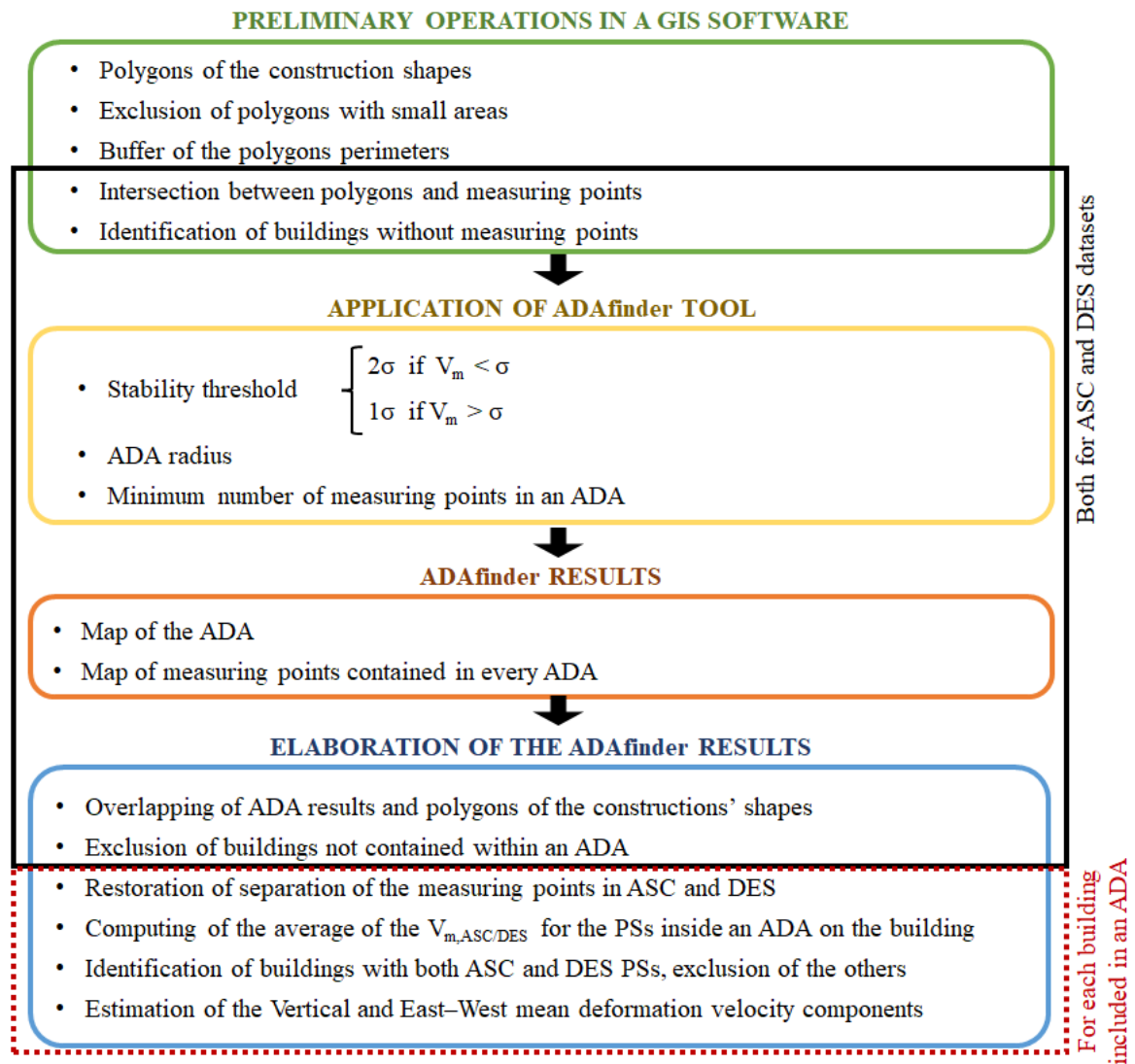

Figure 1: Flowchart of the proposed methodology.

4 APPLICATION

In this Section, the application of the proposed methodology to the case study area is reported. First, a description of the case study area is illustrated. Then, all the steps of the procedure described in Section 3 are explained in detail, with reference to the case study. All the operations are done in QGIS [35].

4.1   Description of the case study area

The case study area, 17 km^2 wide, is part of the industrial zone of the city of Barcelona (Spain) named "Zona Franca". It is located in the South of the city, in the Sants-Montjuïc district. In this area the existing constructions are mainly large sheds, with limited height, and plan roofs. The spatial distribution of the constructions does not follow a geometric pattern. The number of buildings included in the case study area is 1358, and almost half of them have area greater than 1000 m^2.

4.2   Preliminary operations

The shapefile containing the polygons of the constructions shapes has been obtained from OpenStreetMap [36]. The measuring points downloaded by EGMS in the monitored area are represented in Figure 2a and Figure 2b, for ASC and DES orbits, respectively. The V_m are colored using a false color scale, where negative values and positive values mean a movement away or approaching the satellite system, respectively. Looking at these maps, there is an evidence of an ongoing phenomenon in the southern part of the area, while the central and northern part appear to be stable.
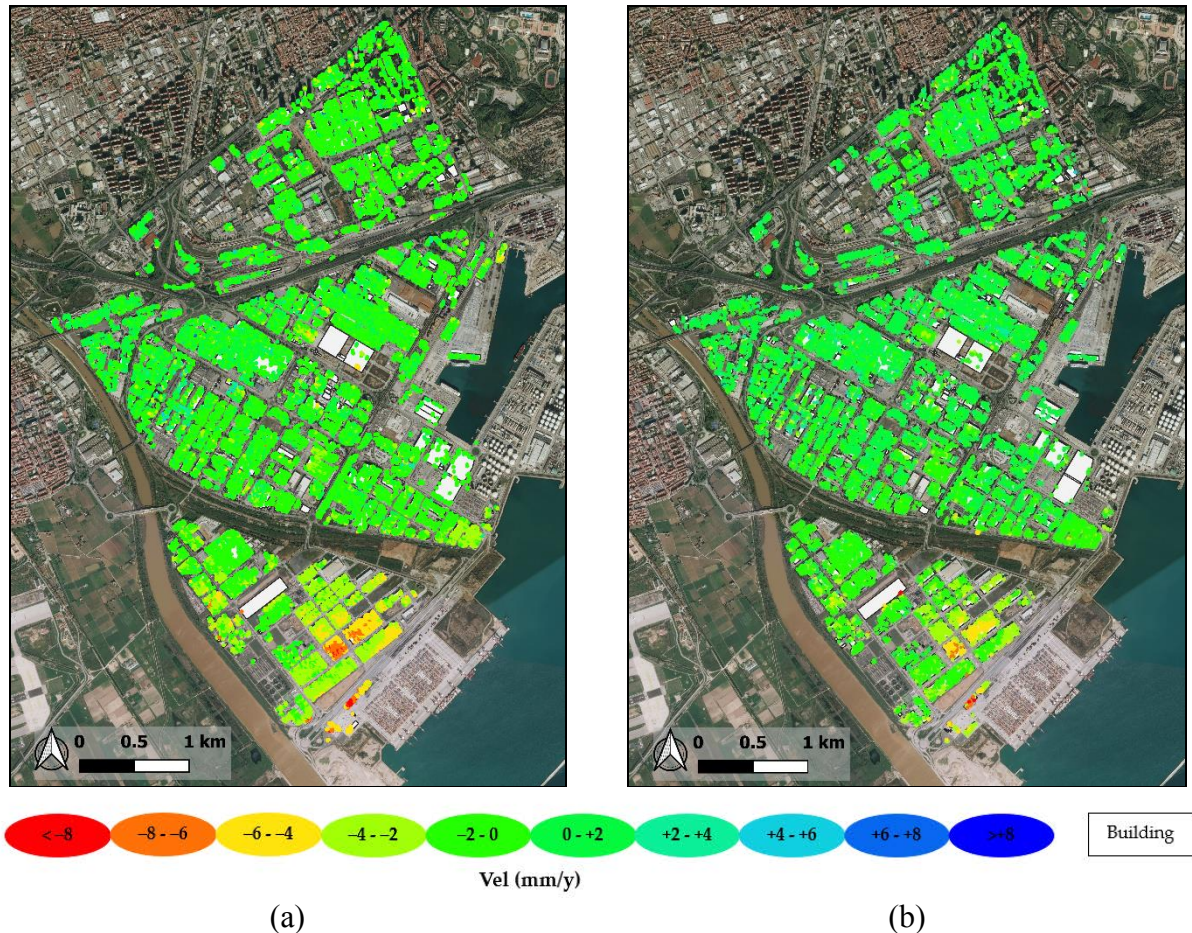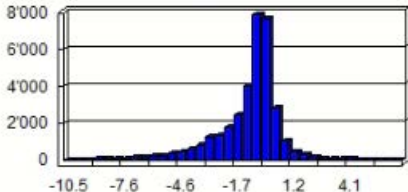

Figure 2: Measuring points on the constructions of the case study area: (a) ascending and (b) descending.

In Table 1 the total number of measuring points and the statistics of their V_m in the case study area are reported, for both datasets. The frequency distribution of V_m has a normal shape. It can be noted that the ASC measuring points are about 75% more than the DES ones and that the V_m is lower that σ. The values of the V_m reach -10.5 mm/y moving away from the
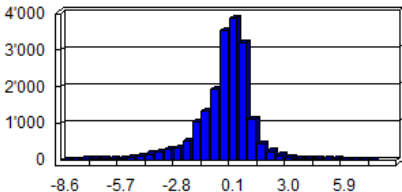
satellite along the ASC LoS. The percentage of constructions without measuring points is 12% for ASC and 18% for DES orbit. Then, the percentage of monitorable buildings, which are covered by both orbits, is the 77%.

Ascending		
Frequency Distribution	Total number	33965
	Minimum V_m	-10.5
	Maximum V_m	6.9
	Average V_m	-0.90
	σ	1.54
Descending		
Frequency Distribution	Total number	19333
	Minimum V_m	-8.6
	Maximum V_m	7.7
	Average V_m	-0.12
	σ	1.35

Table 1: Statistics of the mean velocity V_m of the case study area.

4.3 Application of ADAfinder tool and results

ADAfinder tool is performed using the datasets shown in Figure 2. The threshold value for V_m is 2σ, the radius of the ADA is 25 m, and the minimum number of measuring points is to 3, according to what explained in Section 3. The ADAfinder tool gives a map of the polygonal ADA, and a map of the measuring points included in every ADA. In Figure 3 a focus on the ADA extraction from descending dataset is shown. The distribution of all the PSs on the buildings and the ADA finder results are reported in Figure 3a and Figure 3b, respectively. The PSs are represented with red circular markers, the buildings shapes are white polygons, while the ADA polygons are dark, red-contoured polygons.
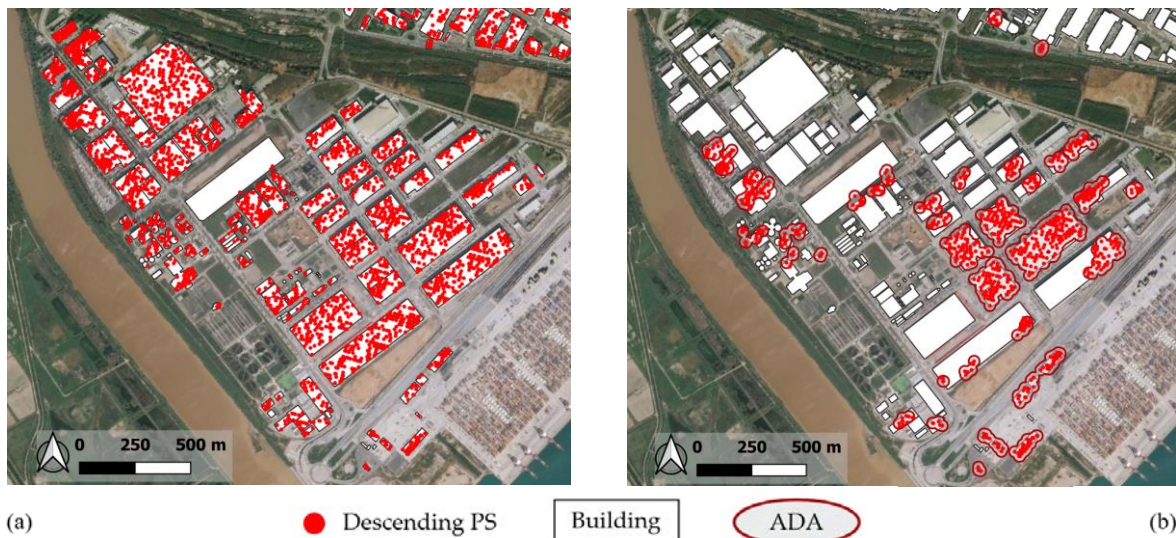

Figure 3: Focus on the ADA extraction from descending dataset: (a) all PSs on the buildings; (b) ADA finder results.

In Figure 4a and Figure 4b, the "active" measuring points, filtered by applying the ADAfinder tool, are reported for ASC and DES orbits, respectively, for the whole area. The V_m is represented using a false colour scale and the same sign convention of the previous Figure 2. Only about the 20% of the initial measuring points is preserved. This was an expected result because of the deformation velocity gradients in the considered portion of the Zona Franca. About 10% of the constructions is included in an ADA.

The statistics of the V_m of the active measuring points, updated on the basis of the ADAfinder results, are reported in Table 2.
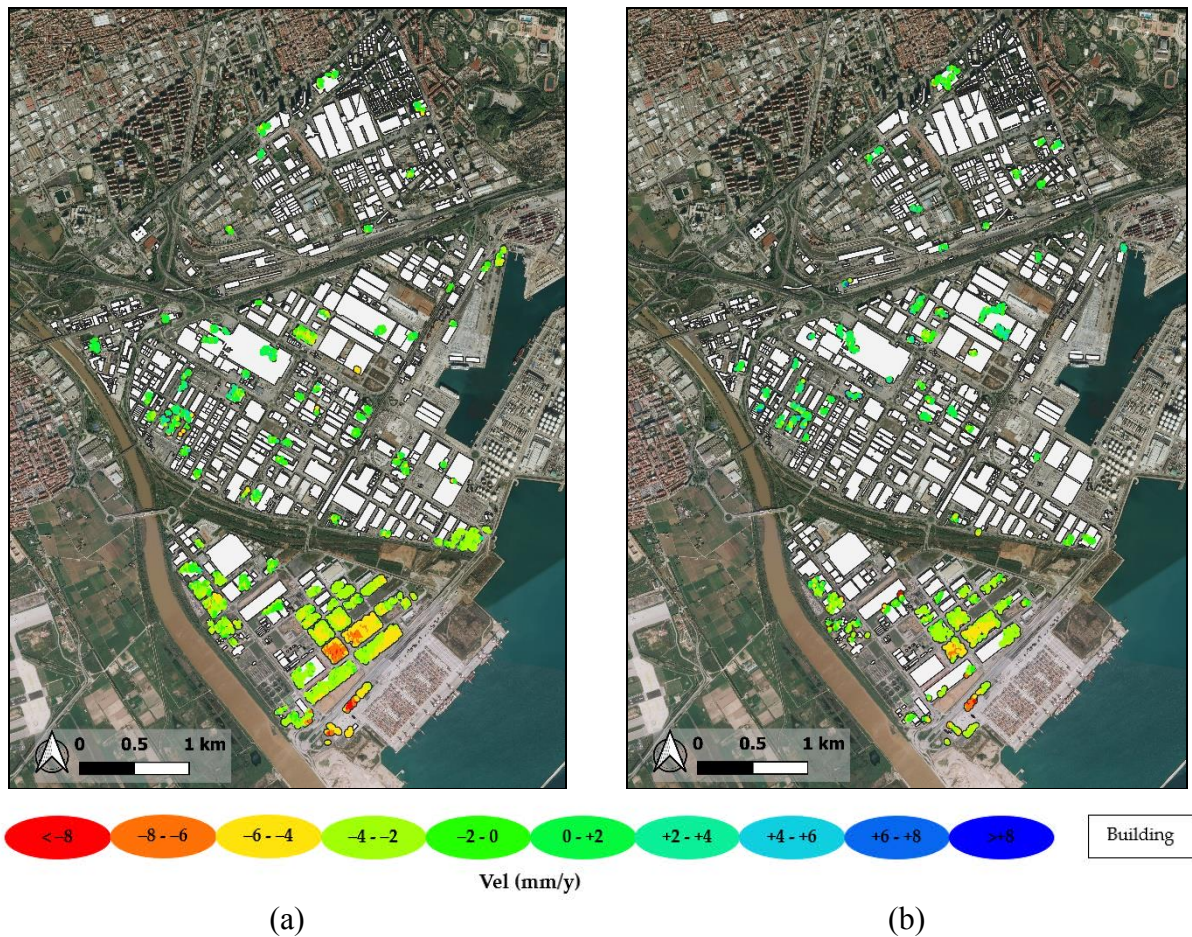

Figure 4: ADA extraction from the active measuring points of the selected area of Zona Franca from (a) ascending and (b) descending datasets.

	Total number	Minimum V_m	Maximum V_m	Average V_m	σ
Ascending	6333	-10.50	6.80	-2.82	2.15
Descending	2248	-8.60	7.70	-1.50	2.49

Table 2: Statistics of the mean velocity V_m of the active measuring points in the case study area.

4.4   Elaboration of the ADAfinder results

The average $V_{m,ASC}$ and $V_{m,DES}$ for each building are shown in Figure 5. The number of measuring points used to compute the $V_{m,ASC/DES}$ for the specific building are reported in labels on these maps. It is important because a greater number of measuring points give a more reliable value. Moreover, the buildings characterized by lack of PSs are covered by black polygons.

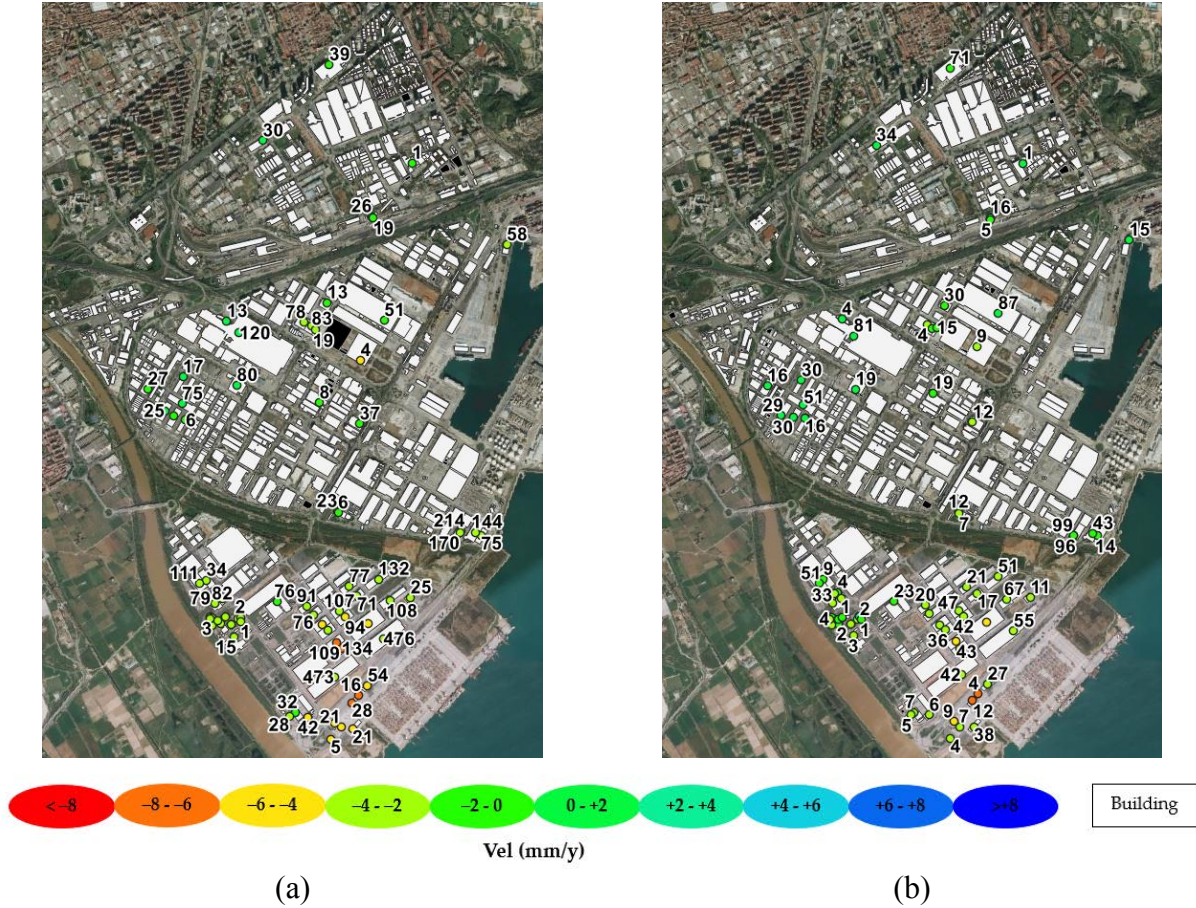(a)   (b)

Figure 5: Maps of buildings in the case study area having an average value of mean deformation velocity along (a) ascending and (b) descending orbit. The black polygons represent buildings without measuring points.

In Figure 6a and Figure 6b, the maps of E-W (V_{EW}) and vertical (V_V) components of the mean deformation velocity are respectively shown. The buildings without measuring points in the original datasets are colored in black. Positive values of V_{EW} and of V_V mean East-directed and upwards-directed displacements, respectively.
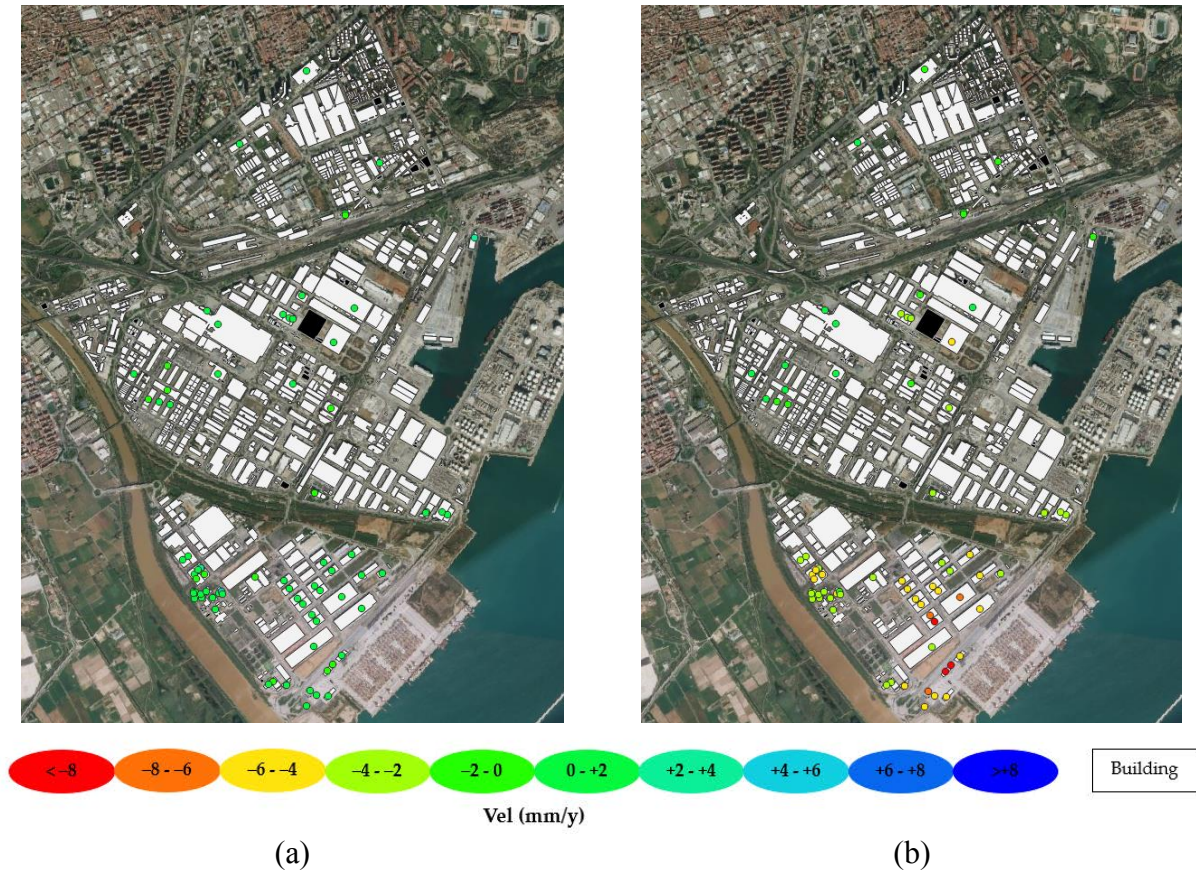
Figure 6: Maps of (a) V_{EW} and (b) V_V components for the "unstable" buildings in the case study area. The black polygons represent buildings without measuring points.

The maps shown in Figure 6a confirm that the southern part of the area presents buildings affected by vertical deformations. Twenty constructions are affected by a vertical velocity included between 4 and 6 mm/y but the values are also greater, with three buildings reaching vertical downward average velocities greater than 8 mm/y.

5 DISCUSSION

In the illustrated procedure, the preliminary operations are necessary to focus on the constructions before the implementation of the ADAfinder tool. In fact, the ADAfinder tool was born for aims quite different from those of this work and has been included in a procedure centered on the SHM. The presented procedure allows to identify the critical constructions on which perform more detailed analyses (e.g., [15], [18],[37]).

The V_{EW} and V_V maps created as a result of the procedure are very synthetic, in fact, one velocity value is associated with every "active" building. This simplification is needed due to the wide dimensions of the areas to monitor (e.g., neighborhoods, municipalities, towns). The evaluation of the two velocity components, vertical and E-W, is important to detect potential ongoing phenomena in the monitored area. In fact, their study can let to the identification of the buildings affected by significant deformations, that need to be additionally monitored.

The procedure proposed and applied in this work exploits EGMS data. Then, it could be repeated yearly, updating the velocity maps based on the update of the EGMS data. In this way, comparisons between the velocity trend could be performed, studying the variation of the velocity values and thinking about fixing thresholds on the maximum acceptable values of variation.

The illustrated application shows that in some cases, there can be constructions without monitoring points, that are not monitorable through satellite-based techniques. However, the lack of measuring points on a construction does not guarantee the absence of displacements. It could be related to the decorrelation effects [38] or anomalies in the deformation signal. The deformation condition of a construction without measuring points can be extrapolated through spatial interpolation of the measuring points in the vicinity if their number and distribution are adequate.

It is worth noting that looking at the initial maps in Figure 2 a and Figure 2 b, a prevailing vertical deformation was supposed to exist, because both the orbits showed negative LoS velocity values, in departure from the satellite, with approximately comparable values.

Particular attention should be paid to the number of measuring points present on the constructions since it affects the reliability of the results (which increases with their number).

6 CONCLUSIONS

In this work, a procedure for the SHM of existing constructions at the territorial scale, using satellite SAR data, is presented. The procedure can be applied using any satellite SAR data, from any satellite constellation, and from any processing techniques. The dataset of measuring points used in this work is given by the EGMS and derives from Sentinel-1 images. Nevertheless, Sentinel-1 data have a low resolution, so, they are useful to monitor large areas. If it is necessary to increase the number of measuring points over the constructions, other SAR satellite data having higher resolution could be used (e.g., those derived by the COSMO-SkyMed constellation).

The procedure allows the identification of buildings affected by velocities above an estimated threshold. It includes the application of the ADAfinder, a new tool that was born to identify ADA in generic areas. The ADAfinder tool is included, for the first time, in a procedure with SHM purposes in urbanized areas or whole municipalities/towns.

The results of the procedure are mean deformation velocity maps, along Vertical and E-W directions, with a value of the component for every building included in an ADA. These maps are very easy to read: the buildings included in ADA require attention and priority in terms of inspections and/or on-site monitoring because they are affected by settlements. For this reason, they could support the management of the safety of urban areas. It is worth highlighting that a limit of the procedure is the impossibility to estimate with accuracy the North–South component of the mean deformation velocity, because of the acquisition geometry of the SAR satellite images.

An application has been presented, for an urbanized area of Barcelona (Spain). The final maps point out the presence of critical constructions in the southern part of the monitored area, affected by prevailing vertical settlements. Many buildings are without measuring points. It is important to take track of them because a lack of measuring points is not always due to the absence of deformation phenomena (other effects could interfere with the acquisition of information).

An improvement of the procedure could be a pre-selection of the typology of buildings to monitor, e.g., based on structural features. In fact, a more accurate velocity threshold specific to each typology could be set.

REFERENCES

[1] Tomás R, Romero R, Mulas JJ, Marturià JJ, Mallorquí JM, Lopez-Sanchez G, et al. (2014) Radar interferometry techniques for the study of ground subsidence phenomena: A review of practical issues through cases in Spain. *Environmental earth sciences,* **71**, 163–181. https://doi.org/10.1007/s12665-013-2422-z.

[2] Crosetto M, Monserrat O, Cuevas-González M, Devanthéry N, Crippa B (2016) Persistent Scatterer Interferometry: a review. ISPRS J Photogramm Remote Sens 115:78–89. https://doi.org/10.1016/j.isprsjprs.2015.10.011

[3] Ferretti A, Prati C, Rocca F, Wasowski J (2006) Satellite interferometry for monitoring ground deformations in the urban environment. In: Proceedings of the 10th IAEG Congress, pp. 100–110

[4] Manunta M, Marsella M, Zeni G, Sciotti M, Atzori S, and Lanari R (2008) Two-scale surface deformation analysis using the SBAS-DInSAR technique: a case study of the city of Rome, Italy, Int J Remote Sens 29(6):1665–1684. 10.1080/01431160701395278

[5] Stramondo S, Bozzano F, Marra F, Wegmuller U, Cinti FR, Moro M, Saroli M (2008) Subsidence induced by urbanisation in the city of Rome detected by advanced InSAR technique and geotechnical investigations. Remote Sensing of Environment, 112(6):3160–3172

[6] Infante D, Confuorto P, Di Martire D, Ramondini M, Calcaterra D (2016) Use of DInSAR data for multi-level vulnerability assessment of urban settings affected by slow-moving and intermittent landslides. Procedia Eng 158:470–475. https://doi.org/10.1016/j.proeng.2016.08.474

[7] Peduto D, Nicodemo G, Maccabiani J, Ferlisi S (2017) Multi-scale analysis of settlement-induced building damage using damage surveys and DInSAR data: a case study in the Netherlands. Eng Geology 218:117-133. https://doi.org/10.1016/j.enggeo.2016.12.018

[8] Mele A, Vitiello A, Bonano M, Miano A, Lanari R, Acampora G, Prota A (2022). On the Joint Exploitation of Satellite DInSAR Measurements and DBSCAN-Based Techniques for Preliminary Identification and Ranking of Critical Constructions in a Built Environment. Remote Sensing, 14(8), 1872.

[9] Costantini M, Ferretti A, Minati F, Falco S, Trillo F, Colombo D, et al. (2017). Analysis of surface deformations over the whole Italian territory by interferometric processing of ERS, Envisat and COSMO-SkyMed radar data. Remote Sens Environ 202:250–275. https://doi.org/10.1016/j.rse.2017.07.017

[10] Arangio S, Calò F, Di Mauro M, Bonano M, Marsella M, Manunta M (2013) An application of the SBAS-DInSAR technique for the assessment of structural damage in the city of Rome. Structure and Infrastructure Engineering: Maintenance, Management, Life-Cycle Design and Performance 10(11):1469-1483. https://doi.org/10.1080/15732479.2013.833949

[11] Bianchini S, Pratesi F, Nolesini T, Casagli N (2015) Building deformation assessment by means of persistent scatterer interferometry analysis on a landslide affected area: The Volterra (Italy) case study. Remote Sensing 7(4):4678-4701. https://doi.org/10.3390/rs70404678

[12] Chen F, Zhou W, Chen C, and Ma P (2019). Extended D-TomoSAR Displacement Monitoring for Nanjing (China) City Built Structure Using High-Resolution TerraSAR/TanDEM-X and Cosmo SkyMed SAR Data. Remote Sensing, 11(22), 2623. https://doi.org/10.3390/rs11222623

[13] Cusson D, Rossi C, Ozkan IF (2021) Early warning system for the detection of unexpected bridge displacements from radar satellite data. J Civ Struct Health Monit 11:189–204. https://doi.org/10.1007/ s13349- 020- 00446-9

[14] Di Carlo F, Miano A, Giannetti I, Mele A, Bonano M, Lanari R, et al. (2021). On the integration of multi-temporal synthetic aperture radar interferometry products and historical surveys data for buildings structural monitoring. J Civ Struct Health Monit 11:1–19. https://doi.org/10.1007/s13349-021-00518-4

[15] Miano A, Mele A, Calcaterra D, Di Martire D, Infante D, Prota A, Ramondini M (2021) The use of satellite data to support the structural health monitoring in areas affected by slow-moving landslides: a potential application to reinforced concrete buildings. Struct Health Monit 20(6): 3265–3287. https://doi.org/10.1177/1475921720983232

[16] Mele A, Miano A, Di Martire D, Infante D, Ramondini M, Prota, A (2022) Potential of remote sensing data to support the seismic safety assessment of reinforced concrete buildings affected by slow-moving landslides. Arch Civ Mech Eng 22(2). 10.1007/s43452-022-00407-7

[17] Miano A, Di Carlo F, Mele A, Giannetti I, Nappo N, Rompato M, et al. (2022) GIS Integration of DInSAR Measurements, Geological Investigation and Historical Surveys for the Structural Monitoring of Buildings and Infrastructures: An Application to the Valco San Paolo Urban Area of Rome. Infrastructures 7(89). https://doi.org/10.3390/infrastructures7070089

[18] Talledo DA, Miano A, Bonano M, Di Carlo F, Lanari R, Manunta M, et al. (2022) Satellite radar interferometry: Potential and limitations for structural assessment and monitoring. J Build Eng 46. 103756. 10.1016/j.jobe.2021.103756

[19] Raspini F, Bianchini S, Ciampalini A, Del Soldato M, Solari L, Novali F, et al. (2018) Continuous, semi-automatic monitoring of ground deformation using Sentinel-1 satellites. Sci Rep 8(1):7253. https://doi.org/10.1038/s41598-018-25369-w

[20] Del Soldato M, Solari L, Raspini F, Bianchini S, Ciampalini A, Montalti R, et al. (2019) Monitoring Ground Instabilities Using SAR Satellite Data: A Practical Approach. ISPRS Int J Geo-Inf 8(7):307. https://doi.org/10.3390/ijgi8070307

[21] Solari L, Del Soldato M, Montalti R, Bianchini S, Raspini F, Thuegaz P, et al. (2019) A Sentinel-1 based hot-spot analysis: landslide mapping in north-western Italy. Int J Remote Sens 40(20):7898–7921. https://doi.org/10.1080/01431161.2019.1607612

[22] Dehls JF, Larsen Y, Marinkovic P, Lauknes TR, Stødle D, Moldestad DA (2019). INSAR. No: A National Insar Deformation Mapping/Monitoring Service In Norway-From Concept To Operations. In: Proceedings of the IGARSS 2019 - 2019 IEEE International Geoscience and Remote Sensing Symposium, pp 5461–5464. 10.1109/IGARSS.2019.8898614

[23] Kalia AC, Frei M, Lege T (2017) A Copernicus downstream-service for the nationwide monitoring of surface displacements in Germany. Remote Sens Env 202:234–249. https://doi.org/10.1016/j.rse.2017.05.015

[24] Crosetto M, Solari L, Balasis-Levinsen J, Casagli N, Frei M, Oyen A, et al. (2020) Ground deformation monitoring at continental scale: the European Ground Motion Service. Int Arch Photogramm Remote Sens Spat Inf Sci 43. https://doi.org/10.5194/isprs-archives-XLIII-B3-2020-293-2020 (b)

[25] https://egms.land.copernicus.eu/

[26] Meisina C, Zucca F, Notti D, Colombo A, Cucchi A, Savio G, et al. (2008) Geological Interpretation of PSInSAR Data at Regional Scale. Sensors 8:7469–7492. https://doi.org/10.3390/s8117469

[27] Bianchini S, Cigna F, Righini G, Proietti C, Casagli N (2012) Landslide HotSpot Mapping by means of Persistent Scatterer Interferometry. Environ Earth Sci 67:1155–1172. https://doi.org/10.1007/s12665-012-1559-5

[28] Raspini F, Bianchini S, Ciampalini A, Del Soldato M, Solari L, Novali F, et al. (2018) Continuous, semi-automatic monitoring of ground deformation using Sentinel-1 satellites. Sci Rep 8:7253. https://doi.org/10.1038/s41598-018-25369-w

[29] Solari L, Barra A, Herrera G, Bianchini S, Monserrat O, Béjar-Pizarro M, et al. (2018) Fast detection of ground motions on vulnerable elements using Sentinel-1 InSAR data. Geomat Nat Hazards Risk 9:152–174. https://doi.org/10.1080/19475705.2017.1413013

[30] Barra A, Solari L, Béjar-Pizarro M, Monserrat O, Bianchini S, Herrera G, et al. (2017) A methodology to detect and update active deformation areas based on sentinel-1 SAR images. Remote Sens 9(10):1002. https://doi.org/10.3390/rs9101002

[31] Navarro JA, Tomás R, Barra A, Pagán JI, Reyes-Carmona C, Solari L, et al. (2020) ADAtools: Automatic detection and classification of active deformation areas from PSI displacement maps. ISPRS Int J Geo-Inf 9(10):584

[32] Tomás R, Pagán JI, Navarro JA, Cano M, Pastor JL, Riquelme A, et al. (2019) Semi-automatic identification and pre-screening of geological–geotechnical deformational processes using persistent scatterer interferometry datasets. Remote Sen 11(14):1675. https://doi.org/10.3390/ijgi9100584

[33] Mele, A., Crosetto, M., Miano, A., Prota., A. (2023). ADAfinder tool applied to EGMS data for the Structural Health Monitoring of urban settlements. Remote Sensing, 15(2), 324.

[34] EGMS White Paper. Available online: https://land.copernicus.eu/user-corner/technical-library/egms-white-paper, accessed on 14 June 2022

[35] QGIS Geographic Information System. QGIS Association. http://www.qgis.org

[36] https://www.openstreetmap.org/, accessed 25/03/2022

[37] Miano, A, Mele, A, Prota, A (2022). Fragility curves for different classes of existing RC buildings under ground differential settlements. Engineering Structures, 257, 114077.

[38] Zebker HA, Villasenor J (1992) Decorrelation in interferometric radar echoes, IEEE Trans Geosci Rem Sens 30:950–959, https://doi.org/10.1109/36.175330